Adsorption of volatile organic compounds by industrial porous materials: Impact of relative humidity

Elwin Hunter-Sellars [a], J.J. Tee [b], Ivan P. Parkin [c], Daryl R. Williams [a,*]

[a] Department of Chemical Engineering, Imperial College London, London, SW7 2AZ, United Kingdom
[b] Procter & Gamble Co., Cincinnati, OH, 45224, USA
[c] Department of Chemistry, University College London, London, WC1E 6BT, United Kingdom

ARTICLE INFO

Keywords:
Competitive adsorption
Volatile organic compound
Water vapour
Hydrophobicity index
Zeolites

ABSTRACT

In this study, the adsorption of several classes of volatile organic compounds by materials with a range of pore size distributions and chemistries were assessed gravimetrically in both dry and wet carrier gas conditions. Measurements carried out at room temperature, and a range of relative humidity values (RH) from 0 to 70%, reflected real-world conditions similar to those of indoor air. Dry removal performance appeared to be dependent on the surface area of adsorbents and, for polar compounds, the relative hydrophobicity of the material. Performance of sorbents with hydrophilic surface chemistry, such as silica gel and molecular sieve 13X, decreased drastically with small increases in pre-exposed humidity. Activated charcoal and high-silica faujasite Y retained their capacities for toluene in relative humidities up to 50% and 70% respectively, with their selectivity for non-polar species credited to hydrophobic pore structure and low water vapour uptake. These conclusions help to emphasise the importance of process humidity as a key parameter when designing or selecting adsorbents in realistic process conditions. Additionally, the methods used in this study provide a simple and reproducible way of testing porous materials for applications requiring or involving high levels of relative humidity.

1. Introduction

Volatile organic compounds (VOCs) are a broad class of chemical species commonly present in waste gas streams from many chemical, petrochemical, and biological sources [1]. Although records vary depending on source and region, the top contributions to airborne VOCs include: refining of mineral oil and gas [2]; industrial production of food, drink, household products, and chemicals [2,3]; and the surface treatment of substances and objects including dyes, paints, and sealants [3,4]. Increased levels of volatile chemicals have been affiliated with a variety of chronic health problems such as asthma [5,6], allergic dermatitis [5], and cancer [5]. However, in recent years it has been hypothesised that the complex mixture of VOCs in indoor air might be a primary cause of several symptoms of 'sick building syndrome' including mucosal irritation, headaches, fatigue, and dizziness [7,8]. The reduction of indoor volatile organic concentrations through adsorption processes is an important research objective, due to its potential to provide improved quality of life for individuals in exposed spaces. Much of this research has been focused on the design and synthesis of porous adsorbents with high surface areas, such as metal organic frameworks [9,10], porous polymers [11], and mixed matrix membranes [12,13]. Despite the vast improvements made in the field of gas adsorbents, materials such as zeolites and activated carbons are ubiquitous in air cleaning applications, due to their low cost and ease of availability.

Many reports exist studying the uptake of VOCs by zeolites [14–16] and carbonaceous [17,18] materials, with studies most commonly carried in dry conditions, or 0% relative humidity (RH). However, water vapour is omnipresent within the environment, and is present in indoor spaces at concentrations several orders of magnitude greater than the concentrations of VOCs. Dynamic studies on zeolitic adsorbents [19,20] and activated carbons [21] have found the presence of humidity has a noticeable impact on the adsorption of gases and volatiles. The common hypothesis among these studies is that the impact of water on adsorbed pollutant quantity depends strongly on the hydrophobicity of the adsorbent, with the presence of hydrophilic bonding sites being found to encourage water adsorption, increasing the degree of competition for volatile species [22]. Developing fast and reproducible methods for the selection or development of materials resistant to pre-exposed water vapour is important to further the field of air cleaning.

This study aims to help bridge the gap between industrial adsorption research on porous materials, commonly performed at 0% RH, and the realistic conditions of air quality applications, by assessing several materials for the removal of harmful species in environmental conditions comparable to indoor air. Adsorbents were chosen based on their high surface area, varying surface chemistry, as well as their popularity in adsorption applications. Activated charcoal, amorphous silica, and both hydrophilic and hydrophobic zeolites were studied for their suitability in adsorbing environmentally relevant species with a range of bonding chemistries. Single component adsorption measurements were carried out gravimetrically to measure the sensitivity of each material to low concentrations of volatile species, typically in the part-per-million range. Two-component gravimetric adsorption measurements with water vapour and volatiles were used to qualitatively assess the impact of pre-exposed ambient humidity on removal performance, to better replicate the real-world conditions these adsorbents would be exposed to in air cleaning applications.

2. Experimental

2.1. Materials

High-silica zeolites zeolite Y (A88Y) and high-silica ZSM-5 (A14Z) were acquired from the PQ Corporation, USA. Molecular sieve 13X (MS13X) and activated charcoal (AC) were acquired from Sigma-Aldrich, USA. Amorphous silica (AS) was acquired from Huber Engineered Materials, USA. All materials were analysed as-received with no modifications, with the exception of drying and activation. All solvent chemicals for vapour generation were ordered with a minimum of 99% purity: toluene and 2-butanone were ordered from Thermo Fisher Scientific, USA; and ethanol was ordered from Sigma-Aldrich, USA. In-house de-ionised water was used for water vapour measurements and humidity pre-conditioning.

2.2. Adsorbent characterisation

X-ray diffraction (XRD) patterns were collected using an X'Pert Pro X-ray diffractometer (Malvern Panalytical, UK) with the following operating conditions: Cu-K_α radiation at 40 kV and 20 mA, in a 2θ scan range of 4°-60°, with a step size of 0.03°. The thermal stability of each sample was assessed using an STA 449 F5 Jupiter (NETZSCH, Germany) to identify any phase transitions or decomposition points that may be encountered during pre-preparation for adsorption measurements. Sample temperatures were raised from 50 to 1000 °C at a rate of 15 °C/min under dry air flow during analysis to test for adsorbent decomposition or the presence of phase transitions. The Si:Al ratios and elemental composition of samples was determined using an Epsilon 3 XLE X-ray fluorescence spectrometer (Malvern Panalytical, UK) with the following operating conditions: Ag anode with maximum settings 50 kV, 3 mA and 15 W; Cu tube filter; Si drift detector, 145 eV @ 5.9 keV/1000 cps.

2.3. Surface area and free space measurements

Surface area and pore volumes of all adsorbents were analysed by low temperature nitrogen sorption, measured at −196 °C using a 3-Flex Physisorption (Micromeritics, USA). Samples weighing 120–200 mg were activated overnight at 300 °C under vacuum overnight prior to analysis, to remove any water or organics present. Brunauer–Emmett–Teller (BET) surface area values were determined using data points in the relative pressure region of $P/P_0 = 0.02–0.07$. Micropore and mesopore volumes were determined using the t-plot and Barrett-Joyner-Halenda (BJH) N_2 desorption models respectively. Pore size distributions were determined from adsorption data using non-linear density functional theory (NLDFT) models, assuming cylindrical pore geometry.

2.4. Single-component adsorption measurements

Adsorption isotherms of all volatile species, as well as water vapour, were carried out gravimetrically using a DVS Endeavour (Surface Measurement Systems, UK) at 25 °C and atmospheric pressure, using 200 mL/min of dry air as the carrier gas for vapour species. Vapour concentrations were measured and maintained using closed-loop control of speed-of-sound (SOS) sensors, with the lowest relative pressure of vapour studied being $P/P_0 = 0.005$. Samples weighing between 40 and 80 mg were activated at 300 °C for 3 h before being held under dry airflow at 25 °C until their masses remained constant.

2.5. Adsorption isotherm model fitting

Experimental adsorption isotherm datasets were fitted using two different data ranges, to better represent the key concentration ranges in the study. Volatiles were fitted in the data range of $P/P_0 = 0–0.20$ using Langmuir, Sips, and Dubinin-Astakhov (DA) models [23], and water vapour was fitted in the data range of P/P_0 using Brunauer-Emmett-Teller (BET) and Guggenheim-Anderson-de Boer (GAB) models [24]. Fitting was carried out through the minimisation of the Marquardt's percent standard deviation (MPSD) [25] calculated between the fitted and experimental values.

2.6. Adsorption measurements under humidity

Humid adsorption measurements utilised the dual-solvent mode of the DVS Endeavour. Following pre-preparation and drying, samples were equilibrated with different levels of humidity, before introducing a step change of $P/P_0 = 0.005$ in volatile concentration while maintaining the same humidity level. The final adsorbed quantity of VOC was calculated by subtracting the mass increase following water adsorption from the total mass uptake of the dry sample in the course of the experiment, assuming no loss of water adsorption. An example of this process, Fig. S1, can be found in the supplementary information. The carrier gas for this process was dry air in all cases, using a total flowrate of 200 mL/min. This experiment represents the 'wet adsorbent' mode of competitive adsorption, where the volatile species bond to unoccupied sites, or attempt to displace pre-adsorbed water present on the material. A similar method has been utilised for studying the impact of humidity on CO_2 adsorption by metal organic frameworks [26,27]. As gravimetric sorption analysis of a two-component vapour stream quantifies the total amount of sorption, any measurements of humid performance must consider this limitation and be considered only semi-quantitative, even when reproducible. In all experiments, the relative pressure of water exceeded that of the VOC by at least 20 times in order to reduce the effect of competition on the reproducibility of results.

2.7. Regeneration of adsorbents under humidity

To test the reusability of porous samples under realistic conditions, adsorption-desorption cycling experiments were carried out using the DVS Endeavour. Cycling of toluene, water, and toluene under the effects of humidity were all tested using similar experimental conditions to the isotherm measurements, using 200 mL/min of dry air at 25 °C, or wet air with a water relative pressure of $P/P_0 = 0.5$ for the two-component cycles, to facilitate regeneration without the use of vacuum or high temperature. Adsorbed quantities were calculated using the change in mass between the ends of the current cycle's adsorption and previous cycle's desorption step.

3. Results and discussion

3.1. Material characterisation

Fig. 1a shows the X-ray diffraction (XRD) patterns for molecular

sieve 13X (MS13X), zeolite Y (A88Y), and ZSM-5 zeolite (A14Z), all of which were compared to, and matched well with, zeolitic reference patterns from the X'Pert HighScore Plus database, indicating that these samples demonstrated a single highly crystalline phase. The similar patterns of MS13X and A88Y are due to the two zeolites having the same faujasite crystal structure, with the two differing in terms of their chemical functionality, with A88Y having a higher framework silica to alumina ratio. Patterns for activated charcoal (AC) and amorphous silica (AS) produced broad peaks and lacked definition due to the materials' amorphous nature. The thermogravimetric mass loss profiles for the adsorbent materials are shown in Fig. 1b. Following initial mass loss in the range T < 200 °C due to surface-bound water and contaminants, all samples were thermally stable up to temperatures around 600 °C in air, confirming that activation could be carried out at any temperature below this point. Past this point, activated charcoal began to thermally degrade, whereas amorphous silica and all zeolites studied were stable until temperatures approaching 1000 °C. MS13X, A88Y, and A14Z were found to have SiO_2:Al_2O_3 ratios of 1.9, 35.8, and 29.7 respectively according to the data collected by x-ray fluorescence. For the high-silica zeolites, this value is lower than the ratio given by the supplier, and is likely due to the presence of extra-framework aluminium or binding agents [28]. AS was found to be over 98.5 mol% SiO_2, with trace amounts of alumina and other metals. XRF could not determine the composition of AC due to its carbonaceous nature. A full summary of elemental compositions can be found in Table S1 of the supplementary information.

The nitrogen adsorption isotherms for the studied sorbents are shown in Fig. 2, with a summary of the results given in Table 1. Activated charcoal was found to have the highest surface area and possessed high pore volumes in both microporous and mesoporous regions. AC's pore structure leads to a network of pores of varying sizes, resulting in a narrow and long hysteresis loop. Faujasites MS13X and A88Y, had similar surface areas, but the latter was found to have a greater fraction of its free space located in mesopores, similar to A14Z. The dealumination process carried out on these zeolites has been shown to create mesopores within the structure of the material [28], which accounts for their comparatively wide hysteresis loops. MS13X, A88Y, and A14Z's specific surface areas were within reported ranges for similar zeolites [29]. Amorphous silica differed from the other sorbents due to its relative lack of micropores, with over 99% of its pore volume located in pores 2 nm or larger. Both AC and AS have surface area values similar to those reported in literature [30,31]. All samples contained pores in suitable size range for adsorbing the volatile species in this study (i.e. above 0.5 nm). Pore size distributions for the five adsorbent samples and comparisons to literature surface area values can be found in Fig. S2 and Table S6 of the supplementary information respectively.

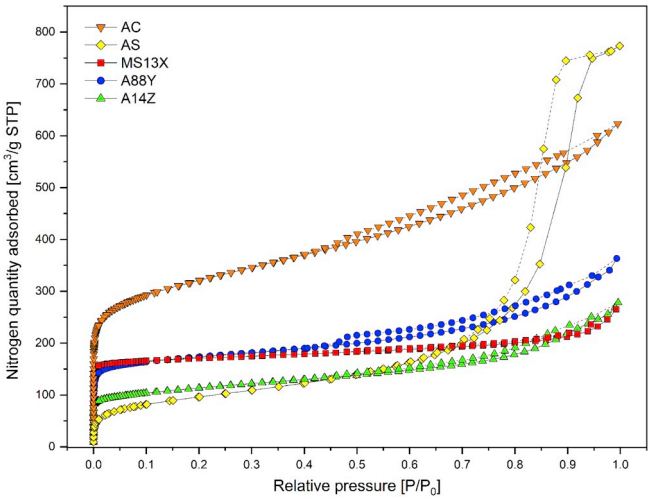

Fig. 2. Nitrogen isotherms for adsorbent samples: activated charcoal, AC; amorphous silica, AS; molecular sieve 13X, MS13X; zeolite Y, A88Y; ZSM-5 zeolite, A14Z. Solid and dashed lines correspond to adsorption and desorption points respectively. T = −196 °C.

Table 1
Surface properties of adsorbents: molecular sieve 13X, MS13X; zeolite Y, A88Y; ZSM-5 zeolite, A14Z; activated charcoal, AC; amorphous silica, AS. Determined using N2 sorption at −196 °C.

Adsorbent	SiO_2:Al_2O_3 [mol/mol]	Surface area [m^2/g]	Micropore volume [cm^3/g]	Mesopore volume [cm^3/g]
AC	N/A	1245	0.210	0.845
AS	>2000[b]	338	0.008	1.187
MS13X	1.9	666	0.209	0.208
A88Y	35.8 (80[a])	659	0.174	0.395
A14Z	29.7 (80[a])	413	0.076	0.318

[a] Quoted from suppliers.
[b] Trace amounts of alumina detected via XRF.

3.2. Single-component adsorption of water and VOCs

Fig. 3a shows the water isotherms for the five studied samples, with the performance of each appearing to depend on both surface chemistry as well as the porosity of the adsorbent. The interaction of adsorbent materials with water molecules is important for indoor air applications due to the prevalence of the latter in these spaces. Molecular sieve 13X was found to be most sensitive to the presence of low levels of humidity, likely due to its high surface area and hydrophilic surface. Amorphous silica, despite its low surface area, adsorbed greater quantities of water than both the high-silica zeolites A14Z and A88Y, and activated

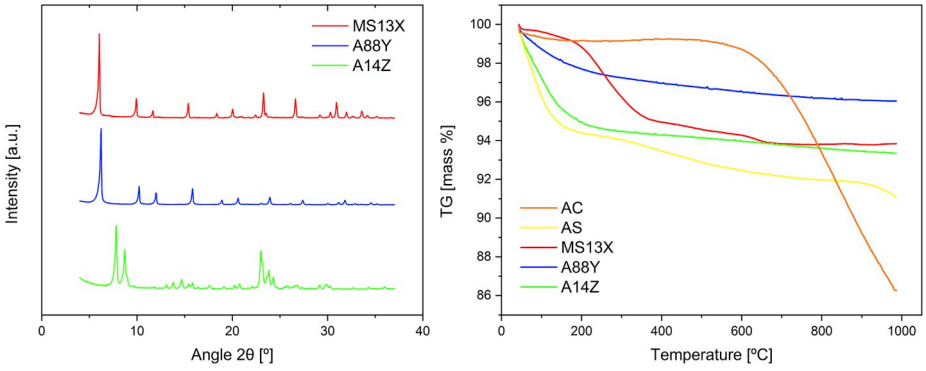

Fig. 1. The (a) X-ray diffraction and (b) thermogravimetric mass loss curves for studied adsorbents: molecular sieve 13X, MS13X; zeolite Y, A88Y; ZSM-5 zeolite, A14Z; activated charcoal, AC; amorphous silica, AS. XRD patterns for activated charcoal and amorphous silica not shown due to amorphous nature.

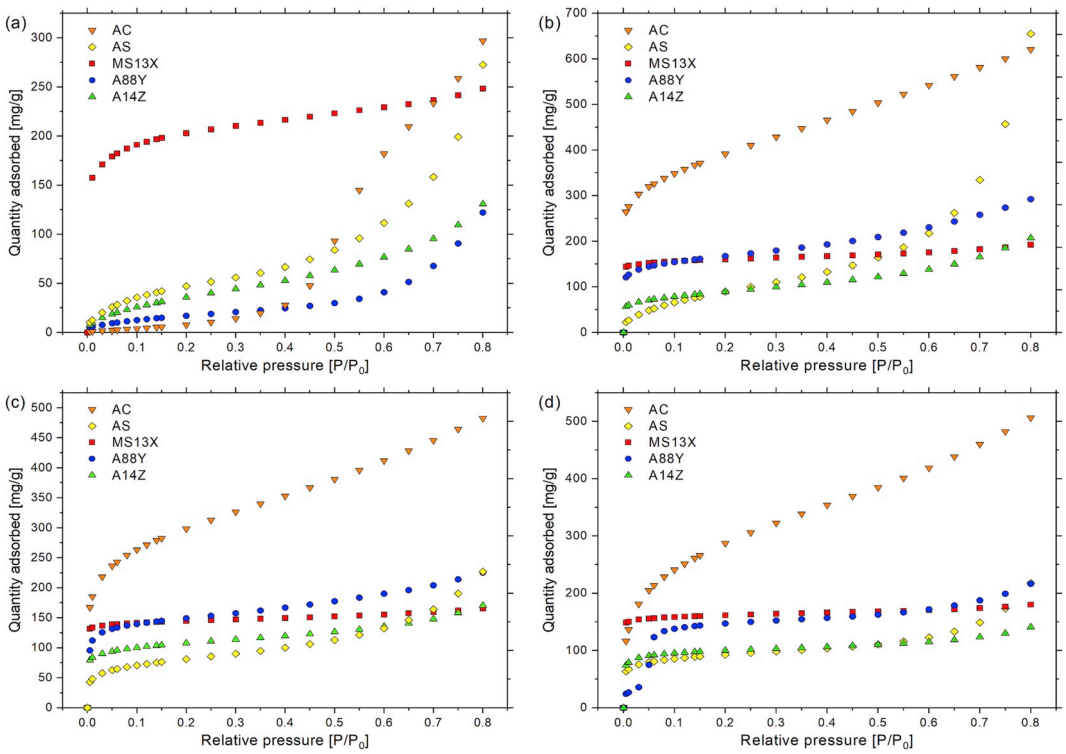

Fig. 3. Gas-solid adsorption isotherms for (a) water, (b) toluene, (c) 2-butanone, and (d) ethanol. Samples studied: activated charcoal, AC; amorphous silica, AS; molecular sieve 13X, MS13X; zeolite Y, A88Y; ZSM-5 zeolite, A14Z. All measurements carried out at atmospheric pressure under dry air flow of 200 mL/min. T = 25 °C.

charcoal, especially at mid-to-high humidity values. Amorphous silica's use as a desiccant is owed to its high water uptake in these humidity ranges, and matches well to literature data for wide-pore silica [32], likely due to its high mesopore volume and lack of hydrophobicity. Despite similar crystal structures, faujasites MS13X and A88Y had notable disparities in their behaviour with water vapour. A88Y and A14Z are designed to have reduced aluminium and sodium cation content, both of which have been attributed to an increase in hydrophobicity in various zeolites [33,34], and are reflected in their water uptake in previous studies [29]. AC had the lowest water uptake initially, followed by an increase at water relative pressures exceeding 0.5 P/P_0 due to the porous nature of the adsorbent, matching well with the trends and absolute quantities reported previously [35]. Higher humidity levels, and corresponding uptakes, are important for adsorption in built environments, as adsorption processes within these locations will typically occur at similar relative humidity levels [36].

The adsorption isotherms of toluene shown in Fig. 3b were best described by type I or type II isotherms, both of which describe rapid micropore filling or surface adsorption at low concentrations [37]. The BET surface area appeared to be a good determinant for the low-pressure adsorption of non-polar species [38], whereas the quantity adsorbed at higher pressures was dependant on the volume of mesopores within the adsorbents. When exposed to 0.005 P/P_0 of toluene, AC was found to possess the highest capacity (264.2 ± 1.2 mg g^{-1}), almost double that of the second-best performer MS13X (145.4 ± 1.6 mg g^{-1}), due to the former's surface area. Good agreement with literature values for low-concentration toluene adsorption was found for AC [39], AS [31], and all zeolites samples [29].

The adsorption of polar species, similarly to water, seemed to be dependent on both the physical and chemical properties of the adsorbent materials. As shown in the low-pressure region of Fig. 3d, AC had a lower capacity for ethanol than MS13X despite the former possessing a higher surface area. Activated charcoals have been found to more readily adsorb non-polar or weakly polar species due to their dispersive bonding chemistry [40]. 2-butanone and ethanol are relatively polar molecules compared to toluene [41] and so, like water, will interact strongly with adsorbents with hydrophilic bonding chemistry such as low-silica molecule sieves [42]. This effect is seen by studying the steepness of the initial stages of the isotherm for AC and A88Y, which decreased noticeably as molecular polarity increases. A88Y formed a stepped type V isotherm when exposed to ethanol, indicating an unfavourable interaction at lower relative pressures. A previous study [43] on methanol and dealuminated zeolites credited this to the difficulty of the polar molecule overcoming the electrostatic barrier of the zeolite Y pores. In this work on ethanol, the 'step' occurs at a lower relative pressure, indicating the repulsion is likely dependant on the electrostatic properties or polarity of the adsorbates. The adsorption of toluene and water onto A88Y provide the two extremes of this interaction: capacity for toluene, due to ease of micropore filling, increases rapidly at low pressure; whereas water is seemingly unable to penetrate this barrier, and is limited to adsorption on the surface or inside the mesopores of A88Y. This reduced capacity for non-polar species due to surface chemistry is a key design constraint for removing VOCs from humidified environments. Polar species such as aldehydes, alcohols, and ketones are some of the most prevalent molecules within built spaces, and contribute significantly to human health and general air quality [44,45]. Therefore, an ideal adsorbent would have sufficient hydrophobicity as to minimise water adsorption but still allow the capture of VOCs with polar bonding chemistries.

3.3. *Fitting of adsorption data to isotherm models*

A range of adsorption isotherm models were used to fit the experimental data in the P/P_0 data ranges of 0–0.2 for volatile species, and 0–0.8 for water vapour. These best represent the concentration ranges of interest for air cleaning and volatile adsorption applications. For brevity, full summaries of fitting parameters for these models can be found in Tables S2–S5 in the supplementary information. For the majority of

volatile species, Dubinin-Astakhov (DA) isotherms provided the best fit of experimental data, followed by Sips model, and finally Langmuir, except in the case of MS13X where the steep initial slope of the experimental isotherm led to difficulties converging the Sips model. The unusual Type V isotherm of the A88Y-ethanol system was described best by the Sips isotherm, as it was capable of fitting the pore-filling inflection point present around $P/P_0 = 0.05$. Experimental data for water uptake was best described by the GAB model for AS, MS13X, and A88Y, and similar errors were found with both GAB and BET for AC and A14Z.

3.4. Hydrophobicity of adsorbents

A summary of the low relative pressure capacities is shown in Table 2, the values of which were used to assess the relative hydrophobicity of each adsorbent through the calculation of hydrophobicity indexes (H.I.) [46]. Several methods for measuring H.I.s exist for both gas and liquid phase adsorption processes, including chemistry [47], energy distributions [48], or wettability [49] of the material's surface using molecular probes with different bonding chemistries. The use of equilibrium adsorption data for calculating indexes has also been outlined in several studies: using dynamic adsorption experiments, where the materials is exposed to the competing species simultaneously [29,50,51]; and static experiments, where the material is exposed to each competing species separately [43,50]. In applications where pre-exposure to humidity is likely, such as passive adsorption processes without the use of active regeneration or a continuous process stream, the additional considerations of dynamic H.I.s (i.e. selectivity based on adsorption kinetics) may not be as pertinent. In this study, indexes were calculated using static adsorption data as a function of process humidity to better understand how humid performance might be linked to the concentration of water vapour. This study defines the hydrophobicity indexes in each system as

$$H.I._{static}(x) = Q_{TOL,\ 0.005} / Q_{H2O,\ x}$$

where $H.I._{static}(x)$ (mol/mol) is the material's static hydrophobicity index at a particular water relative pressure x, $Q_{TOL,\ 0.005}$ (mol/g) is the molar toluene quantity adsorbed by the material at a relative pressure of $P/P_0 = 0.005$, and $Q_{H2O,\ x}$ (mol/g) is the same quantity for water vapour, at a relative pressure of x. In this work, the relative pressure of toluene used for comparison was 0.005 P/P_0, and the relative pressure of water used was varied in order to ascertain how the H.I. value for each adsorbent changed with process humidity, as shown in Fig. 4.

At low humidity, activated charcoal possessed the highest H.I. values, followed by high silica zeolites, and finally amorphous silica and molecular sieve 13X. However, when calculated using water vapour pressure of 0.5 P/P_0, which more accurately represents the relative water and volatile concentrations in indoor air, the H.I. value of zeolite Y was found to be highest. As shown in Fig. 3a, activated charcoal's high mesopore volume leads to an increase in water adsorption when its relative pressure exceeded $P/P_0 = 0.4$, contributing to a steep reduction in its hydrophobicity index in Fig. 4. In the case of zeolite Y, water's interactions are restricted to bonding sites on the surface of the material,

Table 2
Summary of adsorbed vapour amounts by adsorbents: molecular sieve 13X, MS13X; zeolite Y, A88Y; ZSM-5 zeolite, A14Z; activated charcoal, AC; amorphous silica, AS. Determined gravimetrically in single-solvent mode at T = 25 °C.

Adsorbate	Quantity adsorbed [mg/g][a]				
	AC	AS	MS13X	A88Y	A14Z
Water	1.7	10.9	158.1	5.3	8.7
Toluene	264.1	21.2	145.4	120.6	57.4
2-Butanone	167.2	43.0	131.6	95.8	79.5
Ethanol	113.8	61.7	148.2	24.0	73.2

[a] Relative pressure of adsorbate, $P/P_0 = 0.005$.

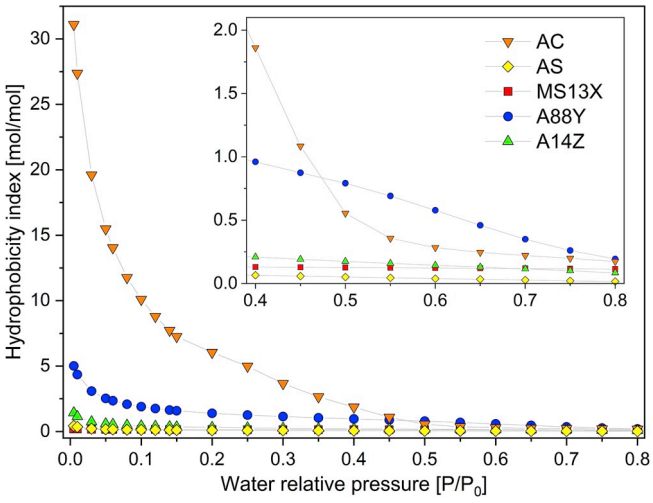

Fig. 4. Hydrophobicity indexes as a function of water relative pressures. His calculated using single-component capacities of toluene at relative pressure of 0.005 P/P_0 and capacities of water vapour at various relative pressures. Inset displays values at water relative pressures exceeding 0.4 P/P0 for clarity. Samples studied: molecular sieve 13X, MS13X; zeolite Y, A88Y; ZSM-5 zeolite, A14Z; activated charcoal, AC; amorphous silica, AS. T = 25 °C.

due to the hydrophobic nature of the adsorbent's pore openings [19,20,43]. These indexes, calculated using single-component adsorption data, may be useful indicators of the performance of adsorbents in the presence of water vapour.

3.5. Impact of humidity on adsorption of toluene and ethanol

Samples were equilibrated with relative pressures of water vapour in the range of $P/P_0 = 0$–0.7 in order to represent both high and low humidity conditions for built environments. The toluene and ethanol removal performance of adsorbents in humid environments, shown in Fig. 5, was found to depend strongly on the hydrophobicity and relative water uptake of the adsorbent. In general, two-component adsorption interactions can be divided into two phenomena: co-adsorption, where the species interact with different adsorption sites; and competitive adsorption, where they occupy and compete for the same adsorption sites. MS13X is the best example for competitive adsorption, as its capacity for both toluene and ethanol dropped to negligible levels following exposure to water vapour. On the other hand, A88Y was found to retain its high adsorption performance for toluene at all humidity values studied. As mentioned previously, the hydrophobic nature of high-silica zeolite pores restrict the adsorption of water molecules to sites on the external surface of the zeolite [19,20,43], allowing water and toluene to co-adsorb onto different bonding sites in the material. Despite A88Y's selectivity for toluene over water, its low capacity for dry ethanol led to similarly low removal in humid conditions. AC's interactions with water and volatile vapour depend on the concentration of water vapour it is exposed to, as predicted by the hydrophobicity indexes calculated previously. At all but the highest humidity, AC maintained a high capacity for both toluene and ethanol despite the presence of water vapour, but its performance was found to decrease noticeably at a relative water pressure of 0.7 P/P_0.

For the adsorption of ethanol, the capacity for A14Z and AS with increasing humidity decreased less severely than for toluene. The polar nature of ethanol could have led to it occupying higher energy adsorption sites unfilled by water molecules. The adsorbed quantity of ethanol for AC appeared to increase at a relative humidity of 30%, which may indicate beneficial adsorbate-adsorbate interactions between pre-adsorbed water molecules and the adsorbing ethanol molecules [52,53]. This interaction likely requires a balance between sufficient surface

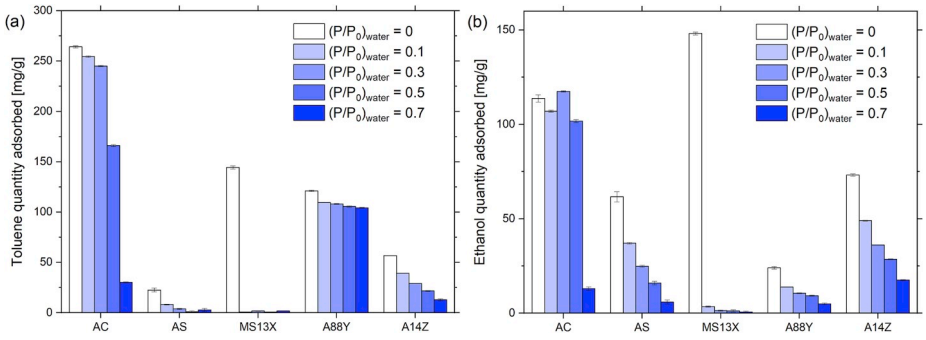

Fig. 5. Adsorption capacities for toluene (a) and ethanol (b) after exposure to humidity, measured using two-solvent gravimetric experiments. Samples studied: activated charcoal, AC; amorphous silica, AS; molecular sieve 13X, MS13X; zeolite Y, A88Y; ZSM-5 zeolite, A14Z. Relative pressure of volatile in all experiments was 0.005 P/P_0.T = 25 °C.

wetting and limited pore blocking as the ethanol capacity was found to decrease at all other humidity values studied. The data collected in single-component measurements appears to offer insight into the performance losses of studied adsorbents. As shown by Fig. 3a, AC's interactions with water vapour begin the transition from type III to type V at relative pressures exceeding 0.5 P/P_0, marked by a sudden increase in water capacity. This point also appears to mark the transition from co-adsorption into competitive adsorption of water vapour and volatiles in Fig. 5, due to the lack of selectivity in the adsorption sites of the studied adsorbent. This decrease in capacity is mirrored in the hydrophobicity indexes plotted in Fig. 4, emphasising the potential use of single-component data in predicting humid adsorption performance.

3.6. Relationship between single- and two-component adsorption measurements

To assess the usefulness of single-component adsorption experiments in predicting performance in realistic conditions, plots were constructed for the relationship between H.I. values and relative toluene adsorbed amounts, calculated using the materials' uptakes under dry and humid conditions. The correlation between single- and two-component results, shown in semi-log plot Fig. 6, was found to be strongest for high-silica zeolites A14Z and A88Y, and activated charcoal, with logarithmic fitting curves having linear regression coefficient (R-squared) values of

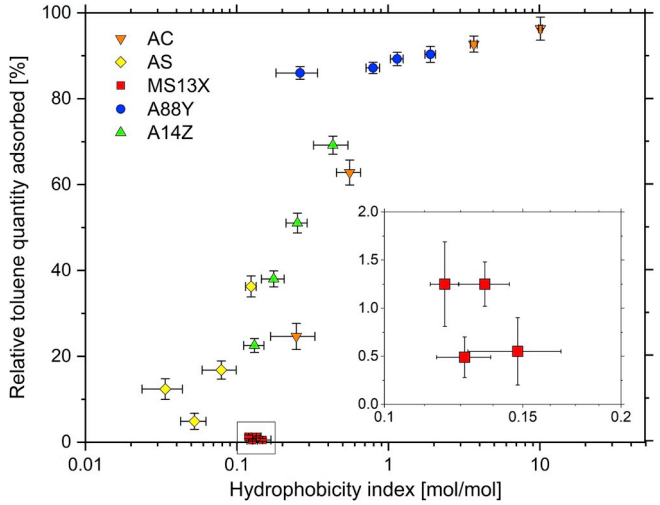

Fig. 6. Relationship between hydrophobicity indexes and toluene uptakes relative to dry experiments, determined gravimetrically using single- and two-component experiments respectively. Samples studied: activated charcoal, AC; amorphous silica, AS; molecular sieve 13X, MS13X; zeolite Y, A88Y; ZSM-5 zeolite, A14Z. T = 25 °C.

0.989, 0.899, and 0.884 respectively. These materials showed a gradual decrease in the amount of toluene they adsorbed, indicating both co-adsorption and competitive adsorption of species, with the exception of A88Y. On the other hand, hydrophilic adsorbents amorphous silica and molecular sieve 13X had weaker correlations with coefficients of 0.649 and 0.198 respectively, the latter of which showed almost no trend between H.I. and relative uptake. There are two possible explanations for these discrepancies in hydrophilic adsorbents: the high relative standard deviations present for low H.I. and relative uptake values lead to a skewing of the data; or indexes calculated using the assumption of co-adsorption were unable to explain the drastic reduction in capacity. Despite these inconsistencies, the results show that data collected from single-component adsorption experiments can provide an insight into performance in humid conditions, in the absence of more complicated or time-intensive experimental techniques.

3.7. Impact of humidity on cycling and regeneration of adsorbents

In all toluene cycling experiments, shown in Fig. 7, adsorbed quantities decreased from cycle 1 to 2 before remaining constant in future cycles. This drop in performance was most noticeable in AC, which had its capacity decrease by around 35%, from 264.2 mg/g to 174.3 mg/g, although this was still noticeably higher than the other adsorbents studied in dry conditions. Regeneration studies on activated charcoal have shown decreases in adsorption capacity with increasing cycle time due to pore blockage, and often utilise high temperature or vacuum conditions for regeneration [54]. In the case of A88Y, the quantity of toluene it adsorbed dropped by around 5% before remaining constant. A similar study on ultra stable (high silica) zeolite Y [55] found its capacity for toluene drop by around 10% in cycling experiments. With the introduction of humidity of $P/P_0 = 0.5$, the amount of toluene adsorbed in the first cycle dropped to the values shown in Fig. 5. AC's relative performance was found to drop by around 35%, identical to that of the dry cycling experiments. A14Z had a drop in performance of around 57%, greater than the drop of ~20% in dry conditions. A88Y maintained a relative performance of over 98% in all studied cycles, allowing it to adsorb quantities of toluene similar to AC under these conditions. The trends observed suggest the role of water vapour in regeneration and adsorption cycling behavior likely depends on the adsorbent's surface chemistry and pore structure, as well as the preferred bonding sites of water and toluene molecules. The negligible amount of toluene adsorbed by AS and MS13X in humid toluene cycling experiments made any accurate analysis difficult.

4. Conclusions

Adsorption measurements were carried out for a number of volatile species relevant in indoor air environments, using five adsorbent materials commonly used in VOC applications. Additionally, the physical

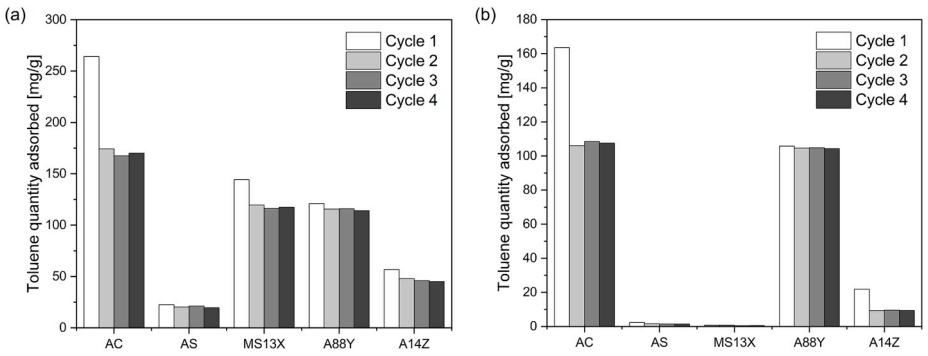

Fig. 7. Quantities of toluene adsorbed as a function of cycle number, under dry (a) and humid (b) conditions. Samples studied: activated charcoal, AC; amorphous silica, AS; molecular sieve 13X, MS13X; zeolite Y, A88Y; ZSM-5 zeolite, A14Z. Relative pressure of toluene in all cycling experiments, $P/P_0 = 0.005$. Relative pressure of water in humid experiments, $P/P_0 = 0.5$. Desorption carried out under 200 mL/min of dry air flow, T = 25 °C.

properties of the adsorbents, such as surface area and micropore volume, were measured using low-temperature nitrogen adsorption. The surface area and microporosity were found to be good indicators for the low-pressure adsorption of non-polar volatiles for all adsorbents. However, these trends did not extend to the polar species studied, as the capacity for these appeared to be a function of both surface chemistry and porosity. Similarly, the adsorption of water vapour at relevantly high humidity was predominantly related to the relative hydrophobicity of the sample, and its degree of mesoporosity to allow for capillary condensation. Future studies quantifying the relative contributions of dispersive and specific energies in adsorbent surfaces could help to predict their adsorption behaviour.

Hydrophobicity indexes, calculated using single-component adsorption data, were able to impart useful information regarding the impact that water vapour may have on VOC removal. These indexes, combined with qualitative trends generated using two-component gravimetric measurements, helped to provide guidelines for the selection of air cleaning adsorbents. MS13X's two-component interactions appeared to be purely competitive, with its uptake for both toluene and ethanol dropping to almost zero following the introduction of water vapour. Even activated charcoal, a commonly used adsorbent for volatiles due to its high surface area and hydrophobicity, had measureable drops in performance when exposed to relative humidity higher than 50%. At the highest humidity values, only high-silica zeolite Y demonstrated a high capacity for toluene due to its hydrophobic micropores and selectivity for non-polar species. However, zeolite Y's low uptake of polar volatiles such as ethanol means a 'catch all' adsorbent with high performance in humid conditions requires additional research. Humid adsorption-desorption regeneration experiments showed interesting behaviour for performance over several cycles, with A14Z having a marked decrease in its VOC desorption efficiencies, while AC and A88Y were largely unaffected. Regardless of the relative performance of the adsorbents tested, this study emphasises the importance of humidity as a key operating condition when assessing the performance of materials for VOC removal, especially in areas where water vapour is present in high concentrations, such as air-cleaning applications.

Author contribution

Declaration of competing interest

The authors declare that they have no known competing financial interests or personal relationships that could have appeared to influence the work reported in this paper.

Acknowledgements

This work was supported by the EPSRC Centre for Doctoral Training in Advanced Characterisation of Materials (Grant Ref: EP/L015277/1).

Appendix A. Supplementary data

References

[1] H. Wang, L. Nie, J. Li, Y. Wang, G. Wang, J. Wang, Z. Hao, Characterization and assessment of volatile organic compounds (VOCs) emissions from typical industries, Chin. Sci. Bull. 58 (2013) 724–730, https://doi.org/10.1007/s11434-012-5345-2.

[2] A. Laurent, M.Z. Hauschild, Impacts of NMVOC emissions on human health in European countries for 2000-2010: use of sector-specific substance profiles, Atmos. Environ. 85 (2014) 247–255, https://doi.org/10.1016/j.atmosenv.2013.11.060.

[3] C. Zheng, J. Shen, Y. Zhang, W. Huang, X. Zhu, X. Wu, L. Chen, X. Gao, K. Cen, Quantitative assessment of industrial VOC emissions in China: historical trend, spatial distribution, uncertainties, and projection, Atmos. Environ. 150 (2017) 116–125, https://doi.org/10.1016/j.atmosenv.2016.11.023.

[4] J. Xing, J. Pleim, R. Mathur, G. Pouliot, C. Hogrefe, C. Gan, C. Wei, Historical gaseous and primary aerosol emissions in the United States from 1990 to 2010, Atmos. Chem. Phys. 13 (2013) 7531–7549, https://doi.org/10.5194/acp-13-7531-2013.

[5] J. Shuai, S. Kim, H. Ryu, J. Park, C.K. Lee, G.-B. Kim, V.U. Ultra Jr., W. Yang, Health risk assessment of volatile organic compounds exposure near Daegu dyeing industrial complex in South Korea, BMC Publ. Health 18 (2018) 1, https://doi.org/10.1186/s12889-018-5454-1.

[6] M.J. Mendell, Indoor residential chemical emissions as risk factors for respiratory and allergic effects in children: a review, Indoor Air 17 (2007) 259–277, https://doi.org/10.1111/j.1600-0668.2007.00478.x.

[7] L. Molhave, Z. Liu, A.H. Jorgensen, O.F. Pedersen, S.K. Kjaegaard, Sensory and physiological effects on humans of combined exposures to air temperatures and volatile organic compounds, Indoor Air 3 (1993) 155–169, https://doi.org/10.1111/j.1600-0668.1993.t01-1-00002.x.

[8] J. Sundell, B. Anderson, K. Anderson, T. Lindvall, Volatile organic compounds in ventilating air in buildings at different sampling points in the buildings and their relationship with the prevalence of occupant symptoms, Indoor Air 3 (1993) 82–93, https://doi.org/10.1111/j.1600-0668.1993.t01-2-00003.x.

[9] K. Vellingiri, P. Kumar, A. Deep, K.H. Kim, Metal-organic frameworks for the adsorption of gaseous toluene under ambient temperature and pressure, Chem. Eng. J. 307 (2017) 1116–1126, https://doi.org/10.1016/j.cej.2016.09.012.

[10] Y. Zheng, F. Chu, B. Zhang, J. Yan, Y. Chen, Ultrahigh adsorption capacities of carbon tetrachloride on MIL-101 and MIL-101/graphene oxide composites, Microporous Mesoporous Mater. 263 (2018) 71–76, https://doi.org/10.1016/j.micromeso.2017.12.007.

[11] Y. Tominaga, T. Kubo, K. Yasuda, K. Kato, K. Hosoya, Development of molecularly imprinted porous polymers for selective adsorption of gaseous compounds,

Microporous Mesoporous Mater. 156 (2012) 161–165, https://doi.org/10.1016/j.micromeso.2012.02.020.
[12] O.G. Nik, X.Y. Chen, S. Kaliaguine, Amine-functionalized zeolite FAU/EMT-polyimide mixed matrix membranes for CO2/CH4 separation, J. Membr. Sci. 379 (2011) 468–478, https://doi.org/10.1016/j.memsci.2011.06.019.
[13] M. Drobek, A. Figoli, S. Santoro, N. Navascués, J. Motuzas, S. Simone, C. Algieri, N. Gaeta, L. Querze, A. Trotta, G. Barbieri, R. Mallada, A. Julbe, E. Drioli, PVDF-MFI mixed matrix membranes as VOCs adsorbers, Microporous Mesoporous Mater. 207 (2015) 126–133, https://doi.org/10.1016/j.micromeso.2015.01.005.
[14] S. Aguado, A.C. Polo, M.P. Bernal, J. Coronas, J. Santamaria, Removal of pollutants from indoor air using zeolite membranes, J. Membr. Sci. 240 (2004) 159–166, https://doi.org/10.1016/j.memsci.2004.05.004.
[15] C.K.W. Meininghaus, R. Prins, Sorption of volatile organic compounds on hydrophobic zeolites, Microporous Mesoporous Mater. 35 (2000) 349–365, https://doi.org/10.1016/S1387-1811(99)00233-4.
[16] S. Brosillon, M.H. Manero, J.N. Foussard, Mass transfer in VOC adsorption on zeolite: experimental and theoretical breakthrough, curves, Environ. Sci. Technol. 35 (2001) 3571–3575, https://doi.org/10.1021/es010017x.
[17] M.A. Sidheswaran, H. Destaillats, D.P. Sullivan, S. Cohn, W.J. Fisk, Energy efficient indoor VOC air cleaning with activated carbon fiber (ACF) filters, Build. Environ. 47 (2012) 357–367, https://doi.org/10.1016/j.buildenv.2011.07.002.
[18] X. Zhang, B. Gao, A.E. Creamer, C. Cao, Y. Li, Adsorption of VOCs onto engineered carbon materials: a review, J. Hazard Mater. 338 (2017) 102–123, https://doi.org/10.1016/j.jhazmat.2017.05.013.
[19] B.S. Bal'zhinimaev, E.A. Paukshtis, A. V Toktarev, E. V Kovalyov, M.A. Yaranova, A.E. Smirnov, S. Stompel, Effect of water on toluene adsorption over high silica zeolites, Microporous Mesoporous Mater. 277 (2019) 70–77, https://doi.org/10.1016/j.micromeso.2018.10.023.
[20] M. Kraus, U. Trommler, F. Holzer, F.D. Kopinke, U. Roland, Competing adsorption of toluene and water on various zeolites, Chem. Eng. J. 351 (2018) 356–363, https://doi.org/10.1016/j.cej.2018.06.128.
[21] J. Rodriguez-Mirasol, J. Bedia, T. Cordero, J. Rodriguez, Influence of water vapor on the adsorption of VOCs on lignin-based activated carbons, Separ. Sci. Technol. 40 (2005) 3113–3135, https://doi.org/10.1080/01496390500385277.
[22] S. Xian, Y. Yu, J. Xiao, Z. Zhang, Q. Xia, H. Wang, Z. Li, Competitive adsorption of water vapor with VOCs dichloroethane, ethyl acetate and benzene on MIL-101(Cr) in humid atmosphere, RSC Adv. 5 (2015) 1827–1834, https://doi.org/10.1039/C4RA10463C.
[23] N. Ayawei, A.N. Ebelegi, D. Wankasi, Modelling and interpretation of adsorption isotherms, J. Chem. 2017 (2017), https://doi.org/10.1155/2017/3039817.
[24] M.S. Alamri, A.A. Mohamed, S. Hussain, M.A. Ibraheem, A.A. Abdo Qasem, Determination of moisture sorption isotherm of crosslinked millet flour and oxirane using GAB and BET, J. Chem. 2018 (2018), https://doi.org/10.1155/2018/2369762.
[25] D.W. Marquardt, An algorithm for least-squares estimation of nonlinear parameters, J. Soc. Ind. Appl. Math. 11 (1963) 431–441, https://doi.org/10.1137/0111030.
[26] V.B. Lopez-Cervantes, E. Sanchez-Gonzalez, T. Jurado-Vazquez, A. Tejeda-Cruz, E. Gonzalez-Zamora, I.A. Ibarra, CO2 adsorption under humid conditions: self-regulated water content in CAU-10, Polyhedron 155 (2018) 163–169, https://doi.org/10.1016/j.poly.2018.08.043.
[27] N. Chanut, S. Bourrelly, B. Kuchta, C. Serre, J.S. Chang, P.A. Wright, P.L. Llewellyn, Screening the effect of water vapour on gas adsorption performance: application to CO2 capture from flue gas in metal–organic frameworks, ChemSusChem 10 (2017) 1543–1553, https://doi.org/10.1002/cssc.201601816.
[28] M.C. Silaghi, C. Chizallet, P. Raybaud, Challenges on molecular aspects of dealumination and desilication of zeolites, Microporous Mesoporous Mater. 191 (2014) 82–96, https://doi.org/10.1016/j.micromeso.2014.02.040.
[29] M. Kraus, U. Trommler, F. Holzer, F. Kopinke, U. Roland, Competing adsorption of toluene and water on various zeolites, Chem. Eng. J. 351 (2018) 356–363, https://doi.org/10.1016/j.cej.2018.06.128.
[30] T. Dobre, O.C. Pârvulescu, G. Iavorschi, M. Stroescu, A. Stoica, Volatile organic compounds removal from gas streams by adsorption onto activated carbon, Ind. Eng. Chem. Res. 53 (2014) 3622–3628, https://doi.org/10.1021/ie402504u.
[31] C.M. Wang, K. Sen Chang, T.-W. Chung, H. Wu, Adsorption equilibria of aromatic compounds on activated carbon, silica gel, and 13X zeolite, J. Chem. Eng. Data 49 (2004) 527–531, https://doi.org/10.1021/je0302102.
[32] R.S. Mikhail, F.A. Shebl, Adsorption in relation to pore structures of silicas II. Water vapor adsorption on wide-pore and microporous silica gels, J. Colloid Interface Sci. 34 (1970) 65–75, https://doi.org/10.1016/0021-9797(70)90259-6.
[33] L. Shirazi, E. Jamshidi, M.R. Ghasemi, The effect of Si/Al ratio of ZSM-5 zeolite on its morphology, acidity and crystal size, Cryst. Res. Technol. 43 (2008) 1300–1306, https://doi.org/10.1002/crat.200800149.
[34] N.Y. Chen, Hydrophobic properties of zeolites, J. Phys. Chem. 80 (1976) 60–64, https://doi.org/10.1021/j100542a013.
[35] S.M. Taqvi, W.S. Appel, M.D. LeVan, Coadsorption of organic compounds and water vapor on BPL activated carbon. 4. Methanol, ethanol, propanol, butanol, and modeling, Ind. Eng. Chem. Res. 38 (1999) 240–250, https://doi.org/10.1021/ie980324k.
[36] A. V Arundel, E.M. Sterling, J.H. Biggin, T.D. Sterling, Indirect health effects of relative humidity in indoor environments, Environ. Health Perspect. 65 (1986) 351–361, https://doi.org/10.1289/ehp.8665351.
[37] M. Thommes, K. Kaneko, A.V. Neimark, J.P. Olivier, F. Rodriguez-Reinoso, J. Rouquerol, K.S.W. Sing, Physisorption of gases, with special reference to the evaluation of surface area and pore size distribution (IUPAC Technical Report), Pure Appl. Chem. 87 (2015) 1051–1069, https://doi.org/10.1515/pac-2014-1117.
[38] W.-H. Tao, T.C.-K. Yang, Y.-N. Chang, L.-K. Chang, T.-W. Chung, Effect of moisture on the adsorption of volatile organic compounds by zeolite 13×, J. Environ. Eng. 130 (2004) 1210–1216, https://doi.org/10.1061/(ASCE)0733-9372(2004)130:10(1210).
[39] M.A. Lillo-Ródenas, A.J. Fletcher, K.M. Thomas, D. Cazorla-Amorós, A. Linares-Solano, Competitive adsorption of a benzene-toluene mixture on activated carbons at low concentration, Carbon N. Y. 44 (2006) 1455–1463, https://doi.org/10.1016/j.carbon.2005.12.001.
[40] M.-H. Lai, R.Q. Chu, H.-C. Huang, S.-H. Shu, T.-W. Chung, Equilibrium isotherms of volatile alkanes, alkenes, and ketones on activated carbon, J. Chem. Eng. Data 54 (2009) 2208–2215, https://doi.org/10.1021/je800826d.
[41] S. Rohani, S. Horne, K. Murthy, Control of product quality in batch crystallization of pharmaceuticals and fine chemicals. Part 1: design of the crystallization process and the effect of solvent, Org. Process Res. Dev. 9 (2005) 858–872, https://doi.org/10.1021/op050049v.
[42] C.M. Shen, W.M. Worek, Cosorption characteristics of solid adsorbents, Int. J. Heat Mass Tran. 37 (1994) 2123–2129, https://doi.org/10.1016/0017-9310(94)90313-1.
[43] I. Halasz, S. Kim, B. Marcus, Hydrophilic and hydrophobic adsorption on Y zeolites, Mol. Phys. 100 (2002) 3123–3132, https://doi.org/10.1080/00268970210133198.
[44] R. Maddalena, M. Russell, D.P. Sullivan, M.G. Apte, Formaldehyde and other volatile organic chemical emissions in four FEMA temporary housing units, Environ. Sci. Technol. 43 (2009) 5626–5632, https://doi.org/10.1021/es9011178.
[45] R. Funaki, S. Tanabe, Chemical emission rates from building materials measured by a small chamber, J. Asian Architect. Build Eng. 1 (2010) 93–100, https://doi.org/10.3130/jaabe.1.2_93.
[46] J. Weitkamp, P. Kleinschmit, A. Kiss, C.H. Berke, The hydrophobicity index – a valuable test for probing the surface properties of zeolitic adsorbents or catalysts, in: Proc. From Ninth Int. Zeolite Conf., Butterworth-Heinemann, 1993, pp. 79–87, https://doi.org/10.1016/B978-1-4832-8383-8.50094-5.
[47] M. Sin, C. Kutzscher, I. Senkovska, T. Ben, S. Qiu, S. Kaskel, E. Brunner, Surface polarity estimation of metal-organic frameworks using liquid-phase mixture adsorption, Microporous Mesoporous Mater. 251 (2017) 129–134, https://doi.org/10.1016/j.micromeso.2017.06.001.
[48] A. Kondor, A. Dallos, Adsorption isotherms of some alkyl aromatic hydrocarbons and surface energies on partially dealuminated Y faujasite zeolite by inverse gas chromatography, J. Chromatogr., A 1362 (2014) 250–261, https://doi.org/10.1016/j.chroma.2014.08.047.
[49] G.P. Hao, Q. Zhang, M. Sin, F. Hippauf, L. Borchardt, E. Brunner, S. Kaskel, Design of hierarchically porous carbons with interlinked hydrophilic and hydrophobic surface and their capacitive behavior, Chem. Mater. 28 (2016) 8715–8725, https://doi.org/10.1021/acs.chemmater.6b03964.
[50] R. Gong, T.C. Keener, A qualitative analysis of the effects of water vapor on multi-component vapor-phase carbon adsorption, Air Waste 43 (1993) 864–872, https://doi.org/10.1080/1073161X.1993.10467169.
[51] Q. Hu, B.J. Dou, H. Tian, J.J. Li, P. Li, Z.P. Hao, Mesoporous silicalite-1 nanospheres and their properties of adsorption and hydrophobicity, Microporous Mesoporous Mater. 129 (2010) 30–36, https://doi.org/10.1016/j.micromeso.2009.08.029.
[52] Z. Shayegan, F. Haghighat, C.S. Lee, A. Bahloul, M. Huard, Effect of surface fluorination of P25-TiO2 on adsorption of indoor environment volatile organic compounds, Chem. Eng. J. 346 (2018) 578–589, https://doi.org/10.1016/j.cej.2018.04.043.
[53] W. Zou, B. Gao, Y.S. Ok, L. Dong, Integrated adsorption and photocatalytic degradation of volatile organic compounds (VOCs) using carbon-based nanocomposites: a critical review, Chemosphere 218 (2019) 845–859, https://doi.org/10.1016/j.chemosphere.2018.11.175.
[54] S.H. Pak, Y.W. Jeon, Effect of vacuum regeneration of activated carbon on volatile organic compound adsorption, Environ. Eng. Res. 22 (2017) 169–174, https://doi.org/10.4491/eer.2016.120.
[55] L. Xu, Y. Li, J. Zhu, Z. Liu, Removal of toluene by adsorption/desorption using ultra-stable Y zeolite, Trans. Tianjin Univ. 25 (2019) 312–321, https://doi.org/10.1007/s12209-019-00186-y.